

Published in final edited form as:

*J Cardiovasc Electrophysiol.* 2014 March ; 25(3): 299–306. doi:10.1111/jce.12327.

## Ibandronate and Ventricular Arrhythmia Risk

Ingrid M. Bonilla<sup>\*</sup>, Pedro Vargas-Pinto, D.V.M., Ph.D.<sup>†</sup>, Yoshinori Nishijima, D.V.M., Ph.D.<sup>\*</sup>, Adriana Pedraza-Toscano, D.V.M., Ph.D.<sup>†</sup>, Hsiang-Ting Ho, Ph.D.<sup>‡,§</sup>, Victor P. Long III, Pharm.D.<sup>\*</sup>, Andriy E. Belevych, Ph.D.<sup>‡,§</sup>, Patric Glynn<sup>§</sup>, Mahmoud Hounsse, M.D.<sup>‡,§</sup>, Troy Rhodes, M.D.<sup>‡,§</sup>, Raul Weiss, M.D.<sup>‡,§</sup>, Thomas J. Hund, Ph.D.<sup>‡,§</sup>, Robert L. Hamlin, D.V.M., Ph.D.<sup>†,§,¶</sup>, Sandor Györke, Ph.D.<sup>‡,§</sup>, and Cynthia A. Carnes, Pharm.D., Ph.D.<sup>\*,†,‡,§</sup>

<sup>\*</sup>College of Pharmacy, the Ohio State University, Columbus, Ohio, USA

<sup>†</sup>College of Veterinary Medicine, the Ohio State University, Columbus, Ohio, USA

<sup>‡</sup>College of Medicine, the Ohio State University, Columbus, Ohio, USA

<sup>§</sup>Dorothy M. Davis Heart and Lung Research Institute, the Ohio State University, Columbus, Ohio, USA

<sup>¶</sup>QTest Labs, Columbus, Ohio, USA

### Abstract

**Introduction**—Bisphosphonates, including ibandronate, are used in the prevention and treatment of osteoporosis.

**Methods and Results**—We report a case of suspected ibandronate-associated arrhythmia, following a single dose of ibandronate in a 55-year-old female. ECG at presentation revealed frequent ectopy and QT/QTc interval prolongation; at follow-up 9 months later the QT/QTc intervals were normalized. Proarrhythmic potential of ibandronate was assessed with a combination of *in vivo* and *in vitro* approaches in canines and canine ventricular myocytes. We observed late onset *in vivo* repolarization instability after ibandronate treatment. Myocytes superfused with ibandronate exhibited action potential duration (APD) prolongation and variability, increased early afterdepolarizations (EADs) and reduced  $I_{to}$  ( $P < 0.05$ ), with no change in  $I_{Kr}$ . Ibandronate-induced APD changes and EADs were prevented by inhibition of intracellular calcium cycling. Ibandronate increased sarcoplasmic reticulum calcium load; during washout there was an increase in calcium spark frequency and spontaneous calcium waves. Computational modeling was used to examine the observed effects of ibandronate. While reductions in  $I_{to}$  alone had modest effects on APD, when combined with altered RyR inactivation kinetics, the model predicted effects on APD and SR  $Ca^{2+}$  load consistent with observed experimental results.

**Conclusion**—Ibandronate may increase the susceptibility to ventricular ectopy and arrhythmias. Collectively these data suggest that reduced  $I_{to}$  combined with abnormal RyR calcium handling may result in a previously unrecognized form of drug-induced proarrhythmia.

Address for correspondence: Cynthia A. Carnes, Pharm.D., Ph.D., College of Pharmacy, 500 W. 12th Avenue, Columbus, OH 43210, USA. Fax: 614-292-1335; carnes.4@osu.edu.

Ingrid M. Bonilla and Pedro Vargas-Pinto contributed equally to the work.

No disclosures.

## Keywords

biophosphonates; calcium; ibandronate; ion channels; long-QT; pharmacology; potassium; proarrhythmia; Torsade de Pointes

---

## Introduction

Bisphosphonates, such as ibandronate, are used in the prevention and treatment of osteoporosis. Osteoporosis is prevalent in postmenopausal women, and bisphosphonates are often used as first-line preventative therapy. Here, we report a suspected case of ibandronate-associated arrhythmia and a subsequent integrated investigation of the proarrhythmic potential of ibandronate.

Cardiotoxicity has been estimated to cause 27% of drug withdrawals from the market, and limits the development of new drug entities.<sup>1</sup> One form of drug-induced proarrhythmia is Torsades de Pointes (TdP), a potentially fatal cardiac arrhythmia that occurs in the setting of prolonged ventricular repolarization. Thus, *in vitro* assessments of arrhythmogenic potential for new drug entities are primarily focused on prolongation of ventricular repolarization, assessed by blockade of  $I_{Kr}$ , the fast component of the delayed rectifier potassium rectifier current in cardiac cells, or blockade of hERG, the human channel protein encoding  $I_{Kr}$ , in heterologous expression systems.<sup>2</sup> Arrhythmogenic potential may also be assessed *in vitro* or *in vivo* in mammals to evaluate prolongation of the QT/QTc on the electrocardiogram (ECG).<sup>3</sup> Beat-to-beat variability of the QT interval or cellular action potential duration (APD) has been suggested as a more reliable predictor of drug induced TdP<sup>4,5</sup> than prolonged repolarization.

While calcium-handling dysregulation in cardiac myocytes is known to contribute to cardiac arrhythmias, as has long been recognized for digitalis glycosides,<sup>6,7</sup> this form of proarrhythmia is not systematically assessed in the drug development process. We examined the effects of ibandronate in a preclinical model, evaluated electrophysiologic and calcium handling effects in isolated myocytes, which was followed by computational modeling to examine the proarrhythmic effects of combined altered repolarization and dysregulated myocyte calcium handling.

## Methods

### Case Report

A 55-year-old woman presented to an outside hospital following a witnessed syncopal episode. Fifteen days prior to the event, she received her first dose of monthly ibandronate; the patient was not taking any other medications. Admission laboratory values were normal except for hypokalemia (3.1 mEq/L). After correction of hypokalemia, her presenting ECG showed a prolonged QTc of 575 milliseconds (Fig. 1A). After transfer to our institution, ventricular ectopy, and nonsustained polymorphic ventricular tachycardia (PMVT) were seen on telemetry. Given her syncopal episode and persistently prolonged QT interval in the absence of a recognized cause for QT prolongation or arrhythmias, an implantable cardioverter-defibrillator (ICD) was placed.<sup>8</sup> Ibandronate therapy was discontinued after the

initial dose. Nine months after initial presentation, her QT and QTc were 400 and 426 milliseconds, respectively (Fig. 1B); no ICD therapies had been administered. Given the normalization of ventricular repolarization following discontinuation of ibandronate, we used preclinical testing to evaluate the proarrhythmic potential of ibandronate.

### Myocyte Isolation

Animal procedures were approved by the Institutional Animal Care and Use Committee of the Ohio State University. Thirty adult mixed breed dogs (male/female, age 9 months to 5 years) weighing between 8 and 20 kg with normal cardiac function were used for the experiments. On the day of the experiment, the dogs were anesthetized with pentobarbital sodium injection (50 mg/kg IV; Nembutal, Abbott Laboratories, Deerfield, IL, USA). The heart was rapidly removed and perfused with cold cardioplegic solution containing the following in mM: NaCl 110, CaCl<sub>2</sub> 1.2, KCl 16, MgCl<sub>2</sub> 16, and NaHCO<sub>3</sub> 10.

Cannulation of the left circumflex was used for the enzymatic myocyte isolation, as previously described.<sup>9</sup> Cells were stored at room temperature until use.<sup>9</sup> This isolation procedure typically yields 70–90% rod shaped ventricular myocytes with clear striations and margins. All myocyte experiments were conducted within 10 hours of isolation.

Amphotericin-B perforated patch clamp techniques were used with a bath temperature of 36 ± 0.5 °C as previously described.<sup>10</sup> Myocytes were placed in a laminin coated cell chamber (Cell Microcontrols, Norfolk, VA, USA) and superfused with bath solution containing (in mM): 135 NaCl, 5 MgCl<sub>2</sub>, 5 KCl, 10 glucose, 1.8 CaCl<sub>2</sub>, and 5 HEPES with pH adjusted to 7.40 with NaOH. Borosilicate glass micropipettes with tip resistance of 1.5–3 MΩ were filled with pipette solution containing the following (in mM): 100 K-aspartate, 40 KCl, 5 MgCl, 5 EGTA, 5 HEPES, and pH adjusted to 7.2 with KOH.

APDs were measured from the average of the last 10 traces (steady state) from a train of 25 action potentials elicited at each stimulation rate. The standard deviation of the APD<sub>90</sub> for the last 10 traces (i.e., from trace 15–25) was used to evaluate repolarization variability.<sup>11</sup> To further evaluate beat to beat variability, Poincaré plots of the last 10 consecutive beats were drawn by plotting each APD<sub>90</sub> (APD<sub>90</sub> n+1) against the APD<sub>90</sub> of the previous beat (APD<sub>90</sub> n) as previously reported.<sup>5</sup> Short-term variability of APD<sub>90</sub>, expressed in milliseconds, was calculated by using the following formula

$\Sigma(\text{APD}_{90n+1} - \text{APD}_{90n})(10 \times \sqrt{2})^{-1}$  as previously reported.<sup>5</sup> Data were collected at baseline, after superfusion with ibandronate (0.01–10 μg/L) and after washout of the drug. Cells demonstrating multiple early afterdepolarizations after drug treatment (Fig. 2, Panel B) were not included in the APD and beat-to-beat variability measurements. EAD propensity was assessed as the percentage of cells exhibiting EADs during ibandronate superfusion and/or washout.

To assess the potential contribution of intracellular calcium handling to the effects of ibandronate, myocytes were incubated in buffer supplemented with BAPTA-AM (10 mM) or ryanodine (100 nM) for at least half-an-hour to either buffer or deplete intracellular calcium, respectively. After incubation, action potentials were recorded as described above, before and after ibandronate (10 μg/L) superfusion.

For potassium current measurements, nifedipine (2  $\mu\text{M}$ ) was added to the bath solution and calcium concentration reduced to 1 mM.<sup>9,11</sup> Only cells with access resistance less than 20 M $\Omega$  were included in the analysis. Data were collected at baseline and after superfusion with 10  $\mu\text{g/L}$  of ibandronate. Voltage protocols are shown in the insets of Figure 2. Data acquisition was performed with a low noise data acquisition system Digidata 1440A (Molecular Devices, Sunnyvale, CA, USA), Clampex 10.2 software and an Axopatch 200A amplifier (Axon Instruments, Sunnyvale, CA, USA).

### Calcium Handling

Calcium transients were measured by Rhod-2 (10  $\mu\text{M}$ ) using an Olympus Fluoview 1000 confocal microscope in line-scan mode. Myocytes were loaded with dye at room temperature and Rhod-2 was excited at 543 nm and fluorescence was collected at wavelength  $>590$  nm. Myocytes were paced by extracellular platinum electrodes at 0.5 Hz for 20 seconds, and recordings made at 0.3 Hz in the presence of 100 nM isoproterenol with external solution containing (in mM): 140 NaCl, 5.4 KCl, 2 CaCl<sub>2</sub>, 0.5 MgCl<sub>2</sub>, 10 HEPES, and 5.6 glucose (pH 7.3). To assess SR Ca<sup>2+</sup> load, 20 mM caffeine was applied at the end of the experiments.

Calcium sparks were studied in myocytes permeabilized with saponin (0.01% for 20–30 seconds) using an internal solution containing the following (in mM): 120 potassium aspartate, 20 KCl, 0.81 MgCl<sub>2</sub>, 1 KH<sub>2</sub>PO<sub>4</sub>, 0.5 EGTA (free [Ca<sup>2+</sup>] $\sim$ 100 nM), 3 MgATP, 10 phosphocreatine, 0.03 Fluo-3 pentopotassium salt, 20 HEPES (pH 7.2), and 5 U/mL–1 creatine phosphokinase.

### Ibandronate Concentrations

The range of *in vitro* ibandronate concentrations were selected to bracket the expected peak and declining unbound plasma concentrations following a single dose.<sup>12</sup> Concentrations were selected with consideration of bioavailability, volume of distribution, and plasma protein binding.<sup>12,13</sup>

### Computational Modeling

A well-validated model of the human ventricular cardiomyocyte was used to simulate ion channel kinetics, action potential, and calcium cycling.<sup>14</sup> Sensitivity analysis was performed, as described,<sup>15</sup> to determine likely candidates for observed changes in AP and SR Ca<sup>2+</sup> load. Briefly, parameters related to SR Ca<sup>2+</sup> release, uptake, and intracellular Ca<sup>2+</sup> homeostasis were perturbed 1 parameter at a time +30% and –30%. APD at 90% repolarization (APD<sub>90</sub>) and maximal diastolic Ca<sup>2+</sup> concentration in the junctional sarcoplasmic reticulum ([Ca<sup>2+</sup>]<sub>JSR</sub>) were determined following steadystate (change in APD  $< 0.1\%$ ) pacing at a cycle length of 1,000 milliseconds. For each property (X) and parameter (p), sensitivity was calculated according to Equation [1] and expressed relative to maximal value for all parameters.

$$S_{X,p} = \frac{X_{p,+30\%} - X_{p,-30\%}}{0.6X_{\text{con}}} \quad (1)$$

## Data Analysis

Canine ECG data were analyzed using an IOX EMKA station. Differences in QTc short-term variability between baseline and 1 month after treatment were tested by Fisher's exact test (Origin 9.0). Cellular electrophysiology data were analyzed using Clampfit 10.3 software (Axon Instruments) and Origin 9.0 software (OriginLab, Northampton, MA, USA). Currents were normalized to cell capacitance in picofarads (pF) and are expressed as pA/pF. Comparisons between baseline and drug-exposed cells were made by the appropriate *t*-test (Origin Pro 9.0, OriginLab). Comparisons between APDs and APD variability at baseline, during ibandronate exposure and during washout were made using one-way ANOVA with post hoc least significant difference testing. (Origin 9.0, OriginLab). Differences in EAD occurrence were tested with Pearson's chi-square test. Differences in Ca<sup>2+</sup> handling were tested by ANOVA. A level of  $P < 0.05$  was accepted as statistically significant. All data are presented as mean  $\pm$  SE and  $P < 0.05$  was the criterion for statistical significance for all comparisons.

## Results

### Ibandronate Effects on Canine QT

Monitoring of canines treated with a single dose of the 3-month intravenous formulation of ibandronate revealed no prolongation of the QT or QTc interval up to 4 weeks post-dosing compared to baseline. However, delayed onset of increased short-term variability of the QTc was observed in 3 of the 4 dogs (Fig. S1) consistent with late-onset drug-induced repolarization instability.

### Cellular Electrophysiology

Treatment of isolated canine ventricular myocytes with ibandronate revealed prolongation of repolarization over a concentration range of 0.01–10  $\mu\text{g/L}$  (Fig. 2), with rate-independent prolongation of APD<sub>50</sub>. The effects of ibandronate were not mitigated by washout, with washout of up to 15 minutes not relieving ( $P < 0.05$  vs baseline) the ibandronate-induced APD<sub>50</sub> prolongation. The effects of ibandronate on APD<sub>90</sub> were similar to those observed in the APD<sub>50</sub>. As observed with the APD<sub>50</sub>, washout of ibandronate did not relieve ibandronate-dependent APD<sub>90</sub> prolongation ( $P < 0.05$  vs baseline).

In addition to the observed ibandronate-induced prolongation of repolarization, a significant ( $P < 0.001$  vs baseline) number of cells exhibited EADs either during drug superfusion (~35%) or washout (~30%, Fig. 2). Notably, no cells exhibited EADs at baseline.

### Potassium Currents

To investigate potential mechanism(s) for ibandronate-induced APD prolongation, we evaluated the effects of drug treatment on major repolarizing K<sup>+</sup> currents. Ibandronate significantly ( $P < 0.05$  vs baseline) reduced  $I_{to}$  slope conductance and the maximal current density (at +50 mV) as shown in Figure 2. Neither  $I_{K1}$  nor  $I_{Kr}$  was affected by ibandronate superfusion (Fig. 2).

## Calcium Depletion and Buffering Experiments

Myocytes were pretreated with ryanodine and then superfused with ibandronate to assess the role of SR calcium release via the ryanodine receptor in ibandronate-dependent cellular proarrhythmia. Repolarization instability was evaluated at an ibandronate concentration of 10  $\mu\text{g/L}$  ibandronate, which is within the expected unbound plasma concentration range.<sup>12</sup> Ryanodine pretreatment prevented ibandronate-dependent increases in APD<sub>50</sub>, APD<sub>90</sub>, beat-to-beat repolarization variability and short-term repolarization variability. ( $P = \text{NS}$  vs baseline, Fig. 3). In addition, experiments were conducted with the calcium chelator, BAPTA. BAPTA pretreatment prevented ibandronate-induced prolongation of APD<sub>50</sub> or APD<sub>90</sub> (Fig. S2). Furthermore, EADs were not observed in either the ryanodine or BAPTA pretreatment experiments (Figs. 3 and S2), suggesting that the arrhythmogenic effects observed after ibandronate treatment are calcium- and RyR dependent.

## Calcium Handling

Superfusion of myocytes with ibandronate did not affect the amplitude of  $\text{Ca}^{2+}$  transients or change the rate of occurrence of spontaneous  $\text{Ca}^{2+}$  waves (Fig. 4B,C). However, ibandronate treatment significantly ( $P < 0.05$  vs baseline and washout) increased the sarcoplasmic reticulum calcium load, assessed from the amplitude of caffeine-induced  $\text{Ca}^{2+}$  transients. Interestingly, ibandronate washout significantly increased the frequency of spontaneous calcium-waves accompanied by a significant ( $P < 0.05$  vs baseline and ibandronate superfusion) decrease in  $\text{Ca}^{2+}$  transient amplitude (Fig. 4). In addition, washout of ibandronate resulted in normalization of the sarcoplasmic reticulum  $\text{Ca}^{2+}$  load.

Calcium sparks were measured with ibandronate (100  $\mu\text{g/L}$ ) in saponin-permeabilized myocytes (Fig. 5). A significant decrease in spark amplitude was observed during ibandronate perfusion ( $P < 0.05$  vs baseline). Ibandronate washout caused a significant increase in the spark frequency (normalized to the SR calcium load) compared to either baseline or ibandronate superfusion ( $P < 0.05$ ).

## Computational Modeling

Computational modeling was used to predict the likely mechanism(s) responsible for the proarrhythmia phenotypes of APD prolongation and increased SR  $\text{Ca}^{2+}$  load observed with ibandronate. Incorporation of the measured defect in  $I_{\text{to}}$  into a human cardiac myocyte model<sup>14</sup> produced only a slight prolongation of APD. Sensitivity analysis was then performed to determine model parameters that had the greatest influence on APD and SR  $\text{Ca}^{2+}$  load. The forward RyR inactivation rate ( $k_{\text{iCa}}$ ) was found to have the greatest effect on APD while also changing SR  $\text{Ca}^{2+}$  load. Combining decreased  $I_{\text{to}}$  with an increase in  $k_{\text{iCa}}$  produced an increase in SR calcium load and prolongation in the action potential similar to the experimentally observed effects (Fig. S3).

## Discussion

Ibandronate is a bisphosphonate used to prevent and treat osteoporosis by increasing bone density and decreasing bone metabolism.<sup>16</sup> Bisphosphonates have been suggested to increase incident atrial fibrillation,<sup>17</sup> although this is not a consistent finding.<sup>18</sup> However, to

our knowledge the syncope and associated QTc prolongation experienced by our patient have not been previously attributed to ibandronate. Together, the normalization of the QTc after ibandronate discontinuation (Fig. 1B), and the lack of arrhythmias requiring ICD therapy during the follow-up period, suggests that the syncopal episode was caused by the drug. While the arrhythmia responsible for the event experienced by the patient is unknown, as there is no concurrent ECG, ventricular arrhythmias were considered as the likely cause based on the patient's presentation.<sup>8</sup> The purpose of this study was to evaluate the possible mechanism(s) behind this rare, but possibly fatal side effect.

Bisphosphonate elimination following intravenous administration is multiphasic.<sup>12</sup> The drug is rapidly distributed into bones and circulating drug is eliminated in the urine. The terminal elimination rate is much slower and occurs as the drug is redistributed from the bone into the blood; some long-term adverse effects of bisphosphonates have been linked to drug redistribution occurring years after discontinuation.<sup>17</sup> Thus, long-term drug redistribution could conceivably contribute to a delayed onset of arrhythmia in the patient case and the delayed *in vivo* response in the canine experiments.

Drug-induced arrhythmias are increasingly recognized to occur during the use of noncardiac drugs. The increased number of recent drug withdrawals due to ventricular arrhythmias suggests that current risk stratification approaches (evaluation of the fast component of the delayed rectifier potassium current [ $I_{Kr}$ ] encoded by the ether a go-go [hERG] channel in isolated cardiac myocytes or heterologous expression systems, and evaluation of ECG recordings with QT prolongation in conscious or anesthetized animals<sup>19</sup>) are not sufficiently sensitive to predict arrhythmic risk. It can take years to decades to detect this rare, but potentially fatal adverse drug effect.<sup>20</sup>

To further investigate the effects of ibandronate on cardiac repolarization and elucidate potential arrhythmia-inducing mechanisms, we used canine ventricular cardiomyocytes. Action potential prolongation is known to be arrhythmogenic by increasing the propensity to develop EADs, which are generally accepted as the most common proximate cause of TdP.<sup>21</sup> The observed ibandronate-induced increase in repolarization instability not only in the action potential but also in intact myocardium, as the QT interval in 3 out of 4 dogs treated with ibandronate demonstrated instability (Fig. S1), are consistent with an increased susceptibility to develop arrhythmias such as TdP.<sup>4</sup>

EAD formation has been also attributed to abnormal calcium release from the SR, which in turn may lead to inward current through the sodium-calcium exchanger (NCX).<sup>22,23</sup> Since calcium-handling abnormalities can also lead to arrhythmia formation,<sup>24,25</sup> we investigated ibandronate effects on calcium handling. Inhibition of calcium cycling by RyR blockade or calcium buffering with ryanodine or BAPTA, respectively, protected the cell from the detrimental effects of ibandronate (i.e., EADs and APD variability). Ibandronate treatment caused a significant increase in calcium load and a decrease in calcium spark amplitude. Drug washout increased the incidence of spontaneous calcium waves, decreased the calcium transient amplitude, and increased calcium sparks. The relationship between intra-SR  $Ca^{2+}$  concentration ( $Ca^{2+}$  load) and  $Ca^{2+}$  release through RyR gating is complicated, as recently reviewed by Radwanski *et al.*<sup>26</sup> At elevated SR  $Ca^{2+}$  loads, the amount of  $Ca^{2+}$  available for

release (fractional SR calcium release) increases. In addition, increased intra-SR  $\text{Ca}^{2+}$  load enhances the frequency of spontaneous calcium release ( $\text{Ca}^{2+}$  sparks).<sup>27</sup> Considered collectively, our data suggest that ibandronate may block the RyR, causing a  $\text{Ca}^{2+}$  load increase. When the drug is washed out, the RyR blockade is relieved, and, coupled with the dynamic increase in SR  $\text{Ca}^{2+}$  load, could result in increased spontaneous calcium waves and spark frequency.

*In silico* experiments using a physiological model of a human ventricular cardiomyocyte to simulate the effects of ibandronate revealed that the drug likely affects multiple targets in the myocyte, including  $I_{\text{to}}$  and RyR calcium release. While the model predicted that either defect alone was insufficient to produce significant APD prolongation and/or increased SR  $\text{Ca}^{2+}$  load, the simulations demonstrate that they have an additive effect that gives rise to the overall phenotype. Thus, proarrhythmia associated with ibandronate may be due to “multiple hits” that act synergistically to alter cell function. The “multiple hit” nature of ibandronate also highlights unique challenges related to screening of drugs for cardiac safety.

### Limitations

This report was initiated by a single case report and it is possible that there were unique patient characteristics that increased susceptibility to late-onset arrhythmias following ibandronate initiation. The myocyte studies were conducted in canine myocytes, while the *in silico* experiments were conducted in a human ventricular cardiomyocyte model. Ion channels and currents vary by species, although there is substantial similarity between humans and canines. The lack of QT prolongation *in vivo*, which contrasts with themyocyte APD prolongation, may have resulted from differences between coupled (*in vivo*) versus uncoupled (*in vitro*) myocytes.

L-type calcium current was not directly measured in these studies, nor was the potential contribution of NCX. The steady-state nature of the *in silico* experiments may have underestimated dynamic effects of calcium dysregulation on INCX, which is accepted as a known contributor to after depolarizations.

### Conclusion

Ibandronate, and possibly other bisphosphonates, may be associated with an unrecognized risk for significant cardiac arrhythmias. Furthermore, the presentation may be insidious with a delayed onset, reducing the likelihood of associating such events with drug exposure. There may be a reduced sensitivity to detect proarrhythmia for drugs that are primarily administered to an older population (i.e., prevention of postmenopausal osteoporosis). The potential for this adverse side effect of ibandronate should be considered, particularly when prescribing the drug to patients with heart abnormalities that may reduce repolarization reserve.

Current testing paradigms to screen for proarrhythmic potential could be strengthened by evaluating beat to beat instability and repolarization reserve in repolarization as well as effects on myocyte calcium handling. Integrated computational modeling of experimental data may also assist in risk stratification for possible proarrhythmic liability. Considered



collectively, our results suggest that evaluation of proarrhythmic risk could be improved, and that the role of ibandronate should be further evaluated in arrhythmia patients.

## Supplementary Material

Refer to Web version on PubMed Central for supplementary material.

## Acknowledgments

The authors thank Ms. Jeanne Green for expert technical assistance and Ms. Jessica Smith for assistance with data analysis.

Support for I.M.B: Supplement to NIH award HL089836; support for T.J.H: NIH HL096805, HL114893.

## References

1. Casartelli A, Lanzoni A, Comelli R, Crivellente F, Defazio R, Dorigatti R, Fasdelli N, Faustinelli I, Pagliaruso S, Tontodonati M, Cristofori P. A novel and integrated approach for the identification and characterization of drug-induced cardiac toxicity in the dog. *Toxicol Pathol.* 2011; 39:361–371. [PubMed: 21422262]
2. Bowes J, Brown AJ, Hamon J, Jarolimek W, Sridhar A, Waldron G, Whitebread S. Reducing safety-related drug attrition: The use of in vitro pharmacological profiling. *Nat Rev Drug Discov.* 2012; 11:909–922. [PubMed: 23197038]
3. Guo L, Dong Z, Guthrie H. Validation of a guinea pig Langendorff heart model for assessing potential cardiovascular liability of drug candidates. *J Pharmacol Toxicol Methods.* 2009; 60:130–151. [PubMed: 19616638]
4. Thomsen MB, Oros A, Schoenmakers M, van Opstal JM, Maas JN, Beekman JD, Vos MA. Proarrhythmic electrical remodelling is associated with increased beat-to-beat variability of repolarisation. *Cardiovasc Res.* 2007; 73:521–530. [PubMed: 17196569]
5. Varkevisser R, Wijers SC, van der Heyden MA, Beekman JD, Meine M, Vos MA. Beat-to-beat variability of repolarization as a new biomarker for proarrhythmia in vivo. *Heart Rhythm.* 2012; 9:1718–1726. [PubMed: 22609158]
6. Wier WG, Hess P. Excitation-contraction coupling in cardiac Purkinje fibers. Effects of cardiotonic steroids on the intracellular  $[Ca^{2+}]$  transient, membrane potential, and contraction. *J Gen Physiol.* 1984; 83:395–415. [PubMed: 6325588]
7. Ho HT, Stevens SC, Terentyeva R, Carnes CA, Terentyev D, Gyorke S. Arrhythmogenic adverse effects of cardiac glycosides are mediated by redox modification of ryanodine receptors. *J Physiol.* 2011; 589(Pt 19):4697–4708. [PubMed: 21807619]
8. Zipes DP, Camm AJ, Borggrefe M, Buxton AE, Chaitman B, Fromer M, Gregoratos G, Klein G, Moss AJ, Myerburg RJ, Priori SG, Quinones MA, Roden DM, Silka MJ, Tracy C, Smith SC Jr, Jacobs AK, Adams CD, Antman EM, Anderson JL, Hunt SA, Halperin JL, Nishimura R, Ornato JP, Page RL, Riegel B, Blanc JJ, Budaj A, Dean V, Deckers JW, Despres C, Dickstein K, Lekakis J, McGregor K, Metra M, Morais J, Osterspey A, Tamargo JL, Zamorano JL. ACC/AHA/ESC 2006 Guidelines for management of patients with ventricular arrhythmias and the prevention of sudden cardiac death: A report of the American College of Cardiology/American Heart Association Task Force and the European Society of Cardiology Committee for Practice Guidelines (writing committee to develop Guidelines for Management of Patients With Ventricular Arrhythmias and the Prevention of Sudden Cardiac Death): Developed in collaboration with the European Heart Rhythm Association and the Heart Rhythm Society. *Circulation.* 2006; 114:e385–e484. [PubMed: 16935995]
9. Sridhar A, Nishijima Y, Terentyev D, Terentyeva R, Uelmen R, Kukielka M, Bonilla IM, Robertson GA, Gyorke S, Billman GE, Carnes CA. Repolarization abnormalities and afterdepolarizations in a canine model of sudden cardiac death. *Am J Physiol Regul Integr Comp Physiol.* 2008; 295:R1463–R1472. [PubMed: 18768760]

10. Sridhar A, da Cunha DN, Lacombe VA, Zhou Q, Fox JJ, Hamlin RL, Carnes CA. The plateau outward current in canine ventricle, sensitive to 4-aminopyridine, is a constitutive contributor to ventricular repolarization. *Br J Pharmacol.* 2007; 152:870–879. [PubMed: 17700726]
11. Bonilla IM, Belevych A, Sridhar A, Nishijima Y, Ho HT, He Q, Kukielka M, Terentyev D, Terentyeva R, Liu B, Long VP, Gyorke S, Carnes CA, Billman GE. Endurance exercise training normalizes repolarization and calcium handling abnormalities preventing ventricular fibrillation in a model of sudden cardiac death. *J Appl Physiol.* 2012; 113:1772–1783. [PubMed: 23042911]
12. Barrett J, Worth E, Bauss F, Epstein S. Ibandronate: A clinical pharmacological and pharmacokinetic update. *J Clin Pharmacol.* 2004; 44:951–965. [PubMed: 15317823]
13. Kimmel DB. Mechanism of action, pharmacokinetic and pharmacodynamic profile, and clinical applications of nitrogen-containing bisphosphonates. *J Dent Res.* 2007; 86:1022–1033. [PubMed: 17959891]
14. Grandi E, Pasqualini FS, Bers DM. A novel computational model of the human ventricular action potential and Ca transient. *J Mol Cell Cardiol.* 2010; 48:112–121. [PubMed: 19835882]
15. Romero L, Pueyo E, Fink M, Rodriguez B. Impact of ionic current variability on human ventricular cellular electrophysiology. *Am J Physiol Heart Circ Physiol.* 2009; 297:H1436–H1445. [PubMed: 19648254]
16. Salari SP, Abdollahi M, Larijani B. Current, new and future treatments of osteoporosis. *Rheumatol Int.* 2011; 31:289–300. [PubMed: 20676643]
17. Salari P, Abdollahi M. Long term bisphosphonate use in osteoporotic patients; A step forward, two steps back. *J Pharm Pharm Sci.* 2012; 15:305–317. [PubMed: 22579009]
18. John CA. Review of the cardiovascular safety of zoledronic acid and other bisphosphonates for the treatment of osteoporosis. *Clin Ther.* 2010; 32:426–436. [PubMed: 20399982]
19. Friedrichs GS, Patmore L, Bass A. Non-clinical evaluation of ventricular repolarization (ICH S7B): Results of an interim survey of international pharmaceutical companies. *J Pharmacol Toxicol Methods.* 2005; 52:6–11. [PubMed: 15975833]
20. Dumotier BM, Georgieva AV. Preclinical cardio-safety assessment of torsadogenic risk and alternative methods to animal experimentation: The inseparable twins. *Cell Biol Toxicol.* 2007; 23:293–302. [PubMed: 17216548]
21. January CT, Moscucci A. Cellular mechanisms of early afterdepolarizations. *Ann N Y Acad Sci.* 1992; 644:23–32. [PubMed: 1562117]
22. Spencer CI, Sham JS. Effects of Na<sup>+</sup>/Ca<sup>2+</sup> exchange induced by SR Ca<sup>2+</sup> release on action potentials and afterdepolarizations in guinea pig ventricular myocytes. *Am J Physiol Heart Circ Physiol.* 2003; 285:H2552–H2562. [PubMed: 12933341]
23. Huffaker R, Lamp ST, Weiss JN, Kogan B. Intracellular calcium cycling, early afterdepolarizations, and reentry in simulated long QT syndrome. *Heart Rhythm.* 2004; 1:441–448. [PubMed: 15851197]
24. Gyorke S, Carnes C. Dysregulated sarcoplasmic reticulum calcium release: Potential pharmacological target in cardiac disease. *Pharmacol Ther.* 2008; 119:340–354. [PubMed: 18675300]
25. Cerrone M, Colombi B, Santoro M, di Barletta MR, Scelsi M, Villani L, Napolitano C, Priori SG. Bidirectional ventricular tachycardia and fibrillation elicited in a knock-in mouse model carrier of a mutation in the cardiac ryanodine receptor. *Circ Res.* 2005; 96:e77–e82. [PubMed: 15890976]
26. Radwanski PB, Belevych AE, Brunello L, Carnes CA, Gyorke S. Storedependent deactivation: Cooling the chain-reaction of myocardial calcium signaling. *J Mol Cell Cardiol.* 2013; 58:77–83. [PubMed: 23108187]
27. Cheng H, Lederer WJ, Cannell MB. Calcium sparks: Elementary events underlying excitation-contraction coupling in heart muscle. *Science.* 1993; 262:740–744. [PubMed: 8235594]

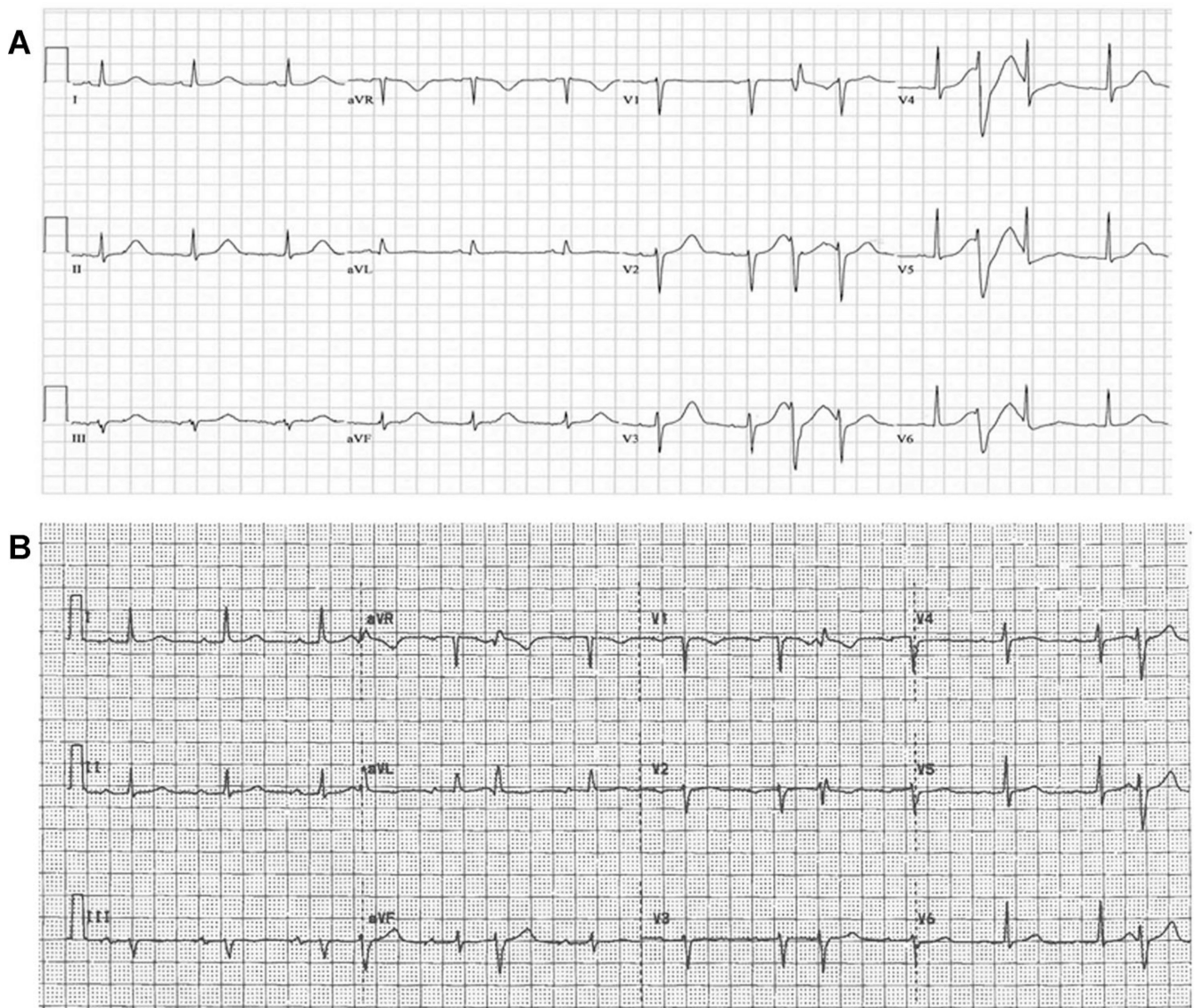


**Figure 1.**

Patient ECG after syncopal episode and 9 months after discontinuation of ibandronate; ibandronate discontinuation normalized the QT interval. A: Electrocardiogram showing ectopic beats, with a prolonged QT interval of 484 milliseconds and Bazett corrected QT interval of 575 milliseconds. ECG was obtained following correction of presenting hypokalemia. B: Repeat electrocardiogram (9 months after initial presentation) showing occasional ectopic beats. The QT interval is 400 milliseconds and the Bazett corrected QT is 426 milliseconds.

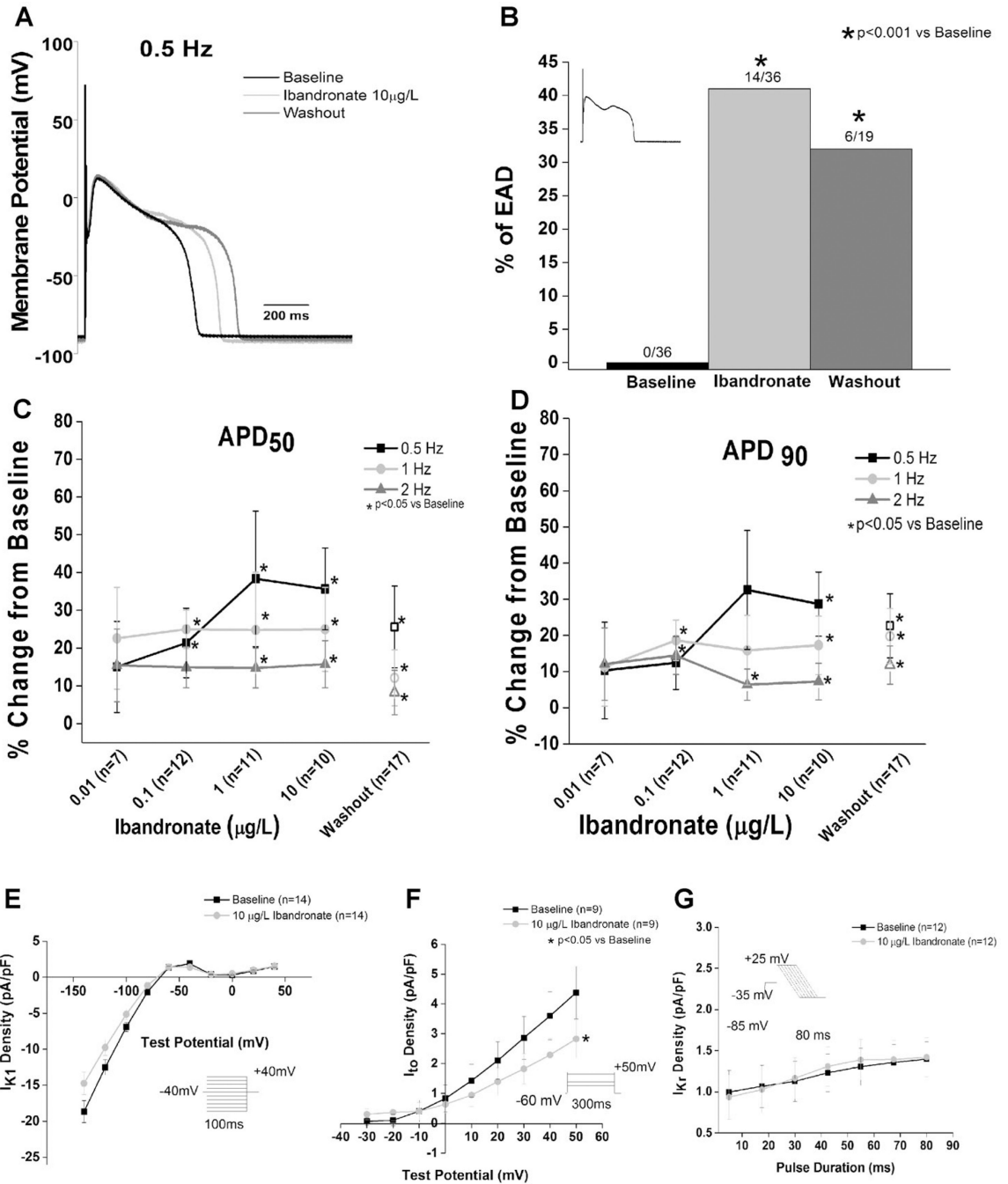


**Figure 2.**

Ibandronate prolongs the action potential, causes EADs, and decreases  $I_{to}$  current density and conductance in left ventricular cardiomyocytes. A: Representative action potential tracings recorded at 0.5 Hz show ibandronate-induced prolongation, which was unrelieved by washout. B: Ibandronate caused a significant increase in the percentage of myocytes with EADs compared to baseline ( $P < 0.001$  vs baseline). The inset shows a representative EAD. Washout of ibandronate did not reduce EADs ( $P < 0.05$  vs baseline). C and D: Ibandronate prolonged the action potential duration at 50 (C) and 90 (D) percent repolarization (closed

symbols). Data shown as percent change from baseline. Open symbols are data obtained during washout. E: No effect of ibandronate on  $I_{K1}$  current density is observed ( $P = NS$  from baseline). F: Ibandronate treatment significantly decreases  $I_{to}$  current density and conductance compared to baseline. ( $P < 0.05$  vs baseline). G: Ibandronate did not alter  $I_{Kr}$  ( $P = NS$  vs baseline). Insets show voltage protocols.

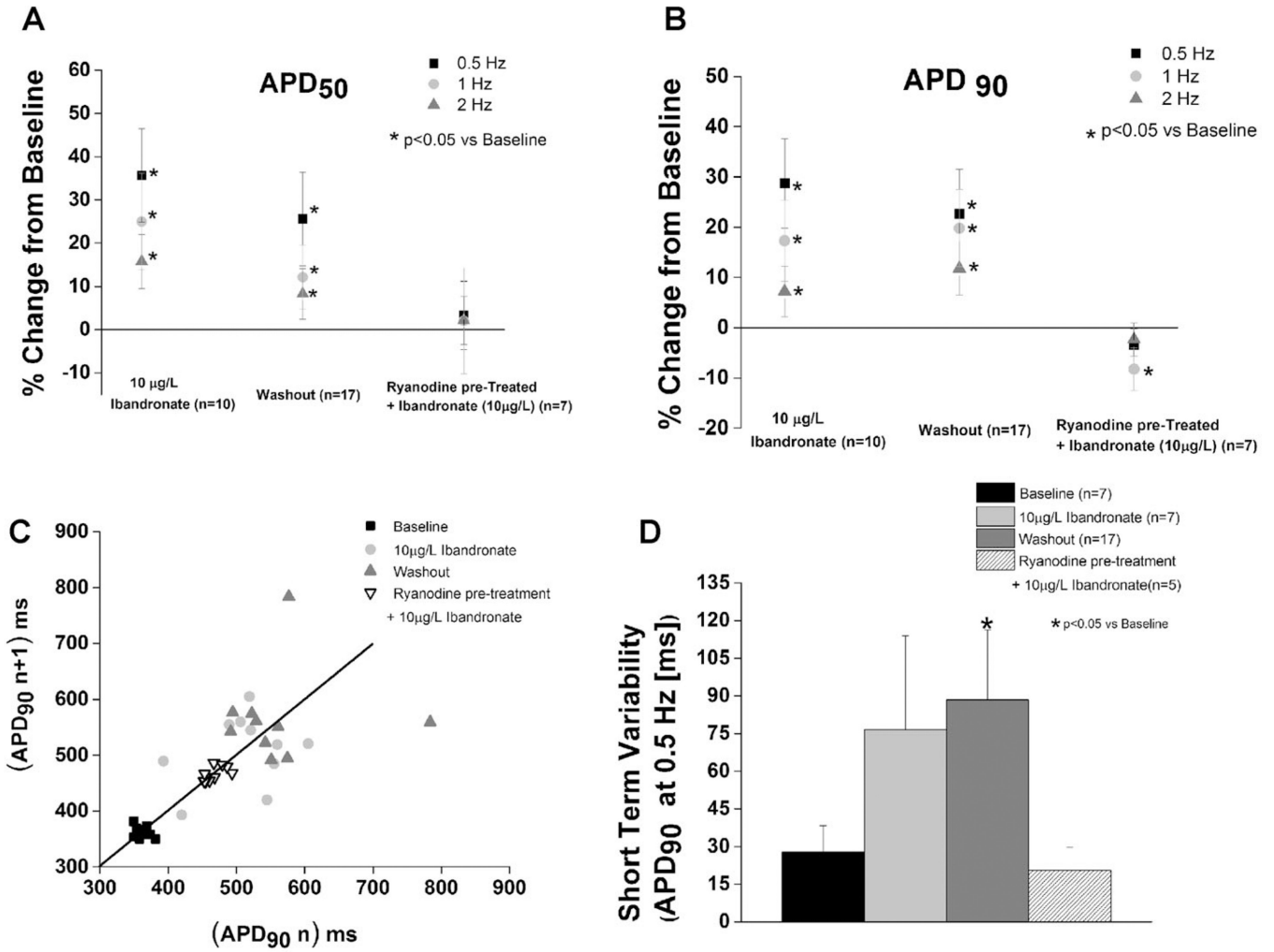


**Figure 3.** Inhibition of calcium cycling prevents ibandronate-induced action potential prolongation and action potential variability. A and B: Ryanodine pretreatment prevented ibandronate-induced prolongation of the action potential and 50% and 90% of repolarization ( $P = NS$  vs baseline). Data presented as percentage change from baseline. C: Representative Poincaré plots of APD<sub>90</sub> during baseline, ibandronate treated, ibandronate washout, and ryanodine pretreated + ibandronate treatment groups. D: Ibandronate washout significantly increases ( $P < 0.05$ ) short-term variability at 0.5 Hz compared to baseline. Ryanodine pretreatment prevented ibandronate-induced increases in short-term variability of APD<sub>90</sub> ( $P = NS$  vs baseline).

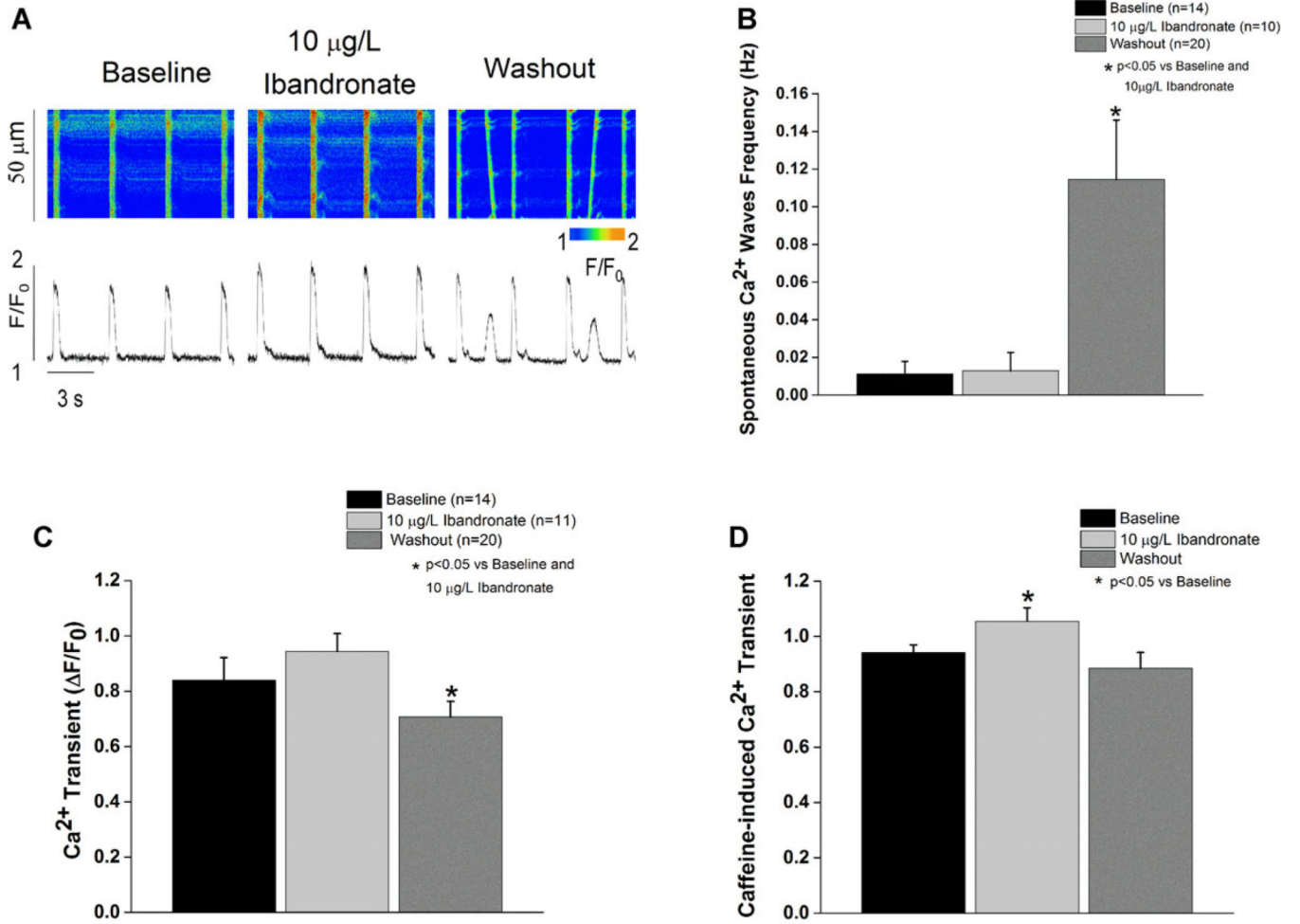


**Figure 4.** Ibandronate treatment increases SR calcium load and washout induces spontaneous calcium waves. **A:** Line scan and tracing representation of calcium transients at baseline, during treatment, and during washout. **B:** Ibandronate washout significantly ( $P < 0.05$ ) increases the spontaneous calcium waves frequency compared to treatment and baseline. **C:** Ibandronate washout significantly ( $P < 0.05$ ) decreases calcium transient amplitude compared to baseline and ibandronate treatment. **D:** Ibandronate treatment significantly ( $P < 0.05$ ) increases SR calcium load defined as caffeine-induced calcium transient compared to baseline.

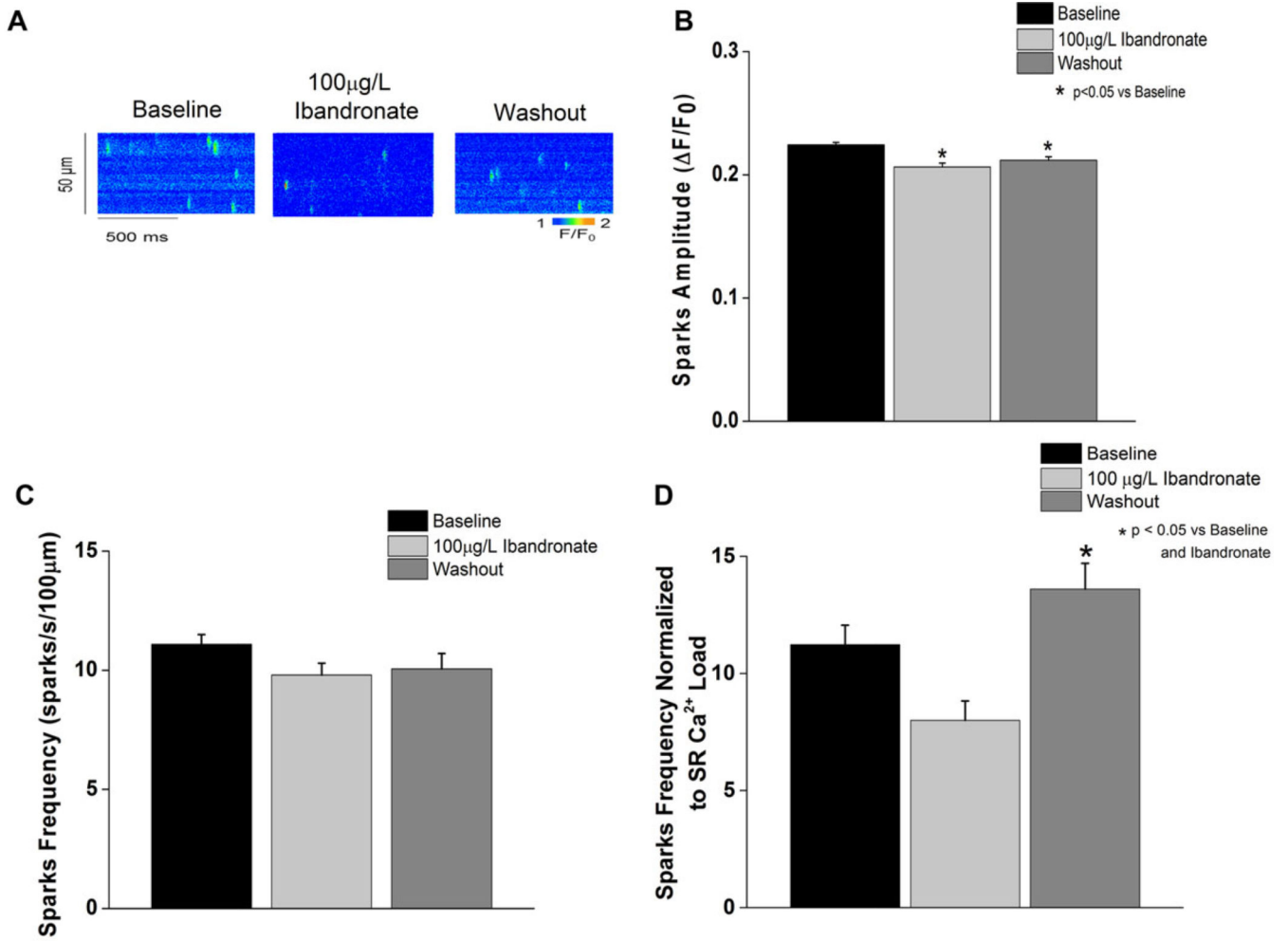


**Figure 5.**

Ibandronate washout increases calcium spark frequency. A: Line scan representation of the calcium spark measured at baseline, during ibandronate treatment, and during washout. B: Ibandronate treatment and washout significantly ( $P < 0.05$ ) decreases calcium spark amplitude compared to baseline. C: Ibandronate treatment and washout did not alter calcium spark frequency. D: Calcium spark frequency, normalized to SR calcium load, was significantly increased during ibandronate washout ( $P < 0.05$ ) compared to baseline and ibandronate treatment.